Journal of Information Systems Engineering and Management
2025, 10(31s)
e-ISSN: 2468-4376
https://www.jisem-journal.com/ **Research Article**

Machine Learning and Numerical Analysis for Predicting and Optimizing Heat Sink Performance in Interrupted Minichannels

I.H. Patel[1]*, A.G. Thakur[2]
[1]*patelih@gmail.com, SVPM's College of Engineering, Malegaon bk,*
[2] *ajay_raja34@yahoo.com, Sanjivani College of Engineering, Kopargaon*

ARTICLE INFO

Received: 26 Dec 2024
Revised: 14 Feb 2025
Accepted: 22 Feb 2025

ABSTRACT

In present research article, researcher investigates geometric modifications in minichannel heat sinks to maximize thermal efficiency while minimizing energy requirements. Main focuses of this study is on interrupted channel designs, where preliminary findings indicate substantial heat transfer improvements using liquid coolants under laminar flow conditions particularly with V-type geometries distributed across channel widths. During the research a comprehensive finite element analysis is conducted to evaluate the thermal performance of various interrupted mini-channel configurations, including rectangular and V-type geometries. Numerical simulations provide insights into key performance metrics, including Reynolds number (Re), Nusselt number (Nu), heat transfer coefficient (h), geometric shape, and flow conditions. After numerical analysis six machine learning models namely Gradient Boosting, Support Vector Regression (SVR), and Ridge Regression, alongside Random Forest, Linear Regression and Lasso Regression are developed to carry out thermal performance optimization. An objective function is formulated to maximize both Nu and h simultaneously. This approach identifies optimal heat sink geometries while revealing performance patterns across different Reynolds number ranges. The research findings provide design guidelines for next-generation minichannel heat sinks with enhanced thermal management capabilities at reduced pumping power requirements.

Keywords: Heat sink, Interrupted channel, Reynolds number (Re), Nusselt number (Nu), Heat transfer coefficient (h), Regression analysis

1. Introduction

A lot of research has been done on mini and microchannel heat sinks in recent decades because of their numerous applications. Copious studies have explored their hydraulic and thermal performance, with a focus on enhancing heat transfer efficiency through different techniques.The thermal management of electronic systems has become increasingly important as device miniaturization continues alongside rising power densities. Mini-channel and micro-channel heat sinks have emerged as prominent solutions for efficient heat dissipation in compact electronic systems.Dixit& Ghosh[1] provided a comprehensive review of micro- and mini-channel heat sinks for single-phase fluids, establishing the foundation for subsequent research. Their work categorized various design considerations and performance parameters, serving as a benchmark for the field. Building upon this foundation, Datta.et al.,[2] expanded the review with emphasis on electronic cooling applications, highlighting the relationship between channel dimensions, flow characteristics, and thermal performance. More recently, Yu, et al.,provided a comprehensive analysis of geometric enhancements for microchannel heat transfer augmentation, classifying various enhancement techniques and their effectiveness. Their review identified key performance metrics and optimization approaches that have guided recent innovations. Researches' consistently shown that channel geometry significantly impacts heat transfer efficiency. Zheng et al.,[4] examined the thermal-hydraulic properties in mini-channels using longitudinal vortex generators with trapezoidal cross sections. Their numerical study demonstrated that these geometries create secondary flows that enhance mixing and heat transfer while maintaining acceptable pressure drops. Similarly, Upadhyay, et al.,[5] conducted a numerical investigation on heat transfer in micro-channels with trapezoidal ribs. Their

research demonstrated how these geometric changes cause the barrier layer to be disrupted, improving the heat transfer coefficients.Xu, et al.,[6] explored experimental and numerical investigations of heat transfer for two-layered microchannel heat sinks under non-uniform heat flux conditions. Their findings demonstrated that layered structures could effectively address thermal management challenges in scenarios with variable heat loads. Naqiuddin, et al.,[7,8] studied geometrically graded micro-channel heat sinks for high heat flux applications, revealing that variable channel dimensions along the flow direction could optimize both heat augmentation and pressure drop characteristics. This work was further developed in their 2018 study, where they used Taguchi-Grey optimization methods to determine optimal configurations for segmented micro-channel heat sinks. Liu & Yu[9] conducted a numerical study on the performance of mini-channel heat sinks with non-uniform inlets. Their research demonstrated that inlet configuration significantly affects flow distribution and, consequently, thermal performance. By optimizing inlet geometries, they achieved more uniform temperature distributions and enhanced heat transfer.Lori&Vafai[10]analyzed heat transfer and fluid flow in microchannel heat sinks with periodic vertical porous ribs. Their work demonstrated that strategically placed porous structures could significantly enhance mixing and heat transfer while maintaining manageable pressure drops. The introduction of porous media created secondary flows and disrupted thermal boundary layers, leading to substantial performance improvements.

Sushma, et al.,[11] investigated the enhancement of heat transfer characteristics in plain fins coated with graphene nanoparticles. Their experimental results showed significant improvements in thermal conductivity and heat transfer rates, suggesting that surface modifications at the nanoscale offer promising avenues for performance enhancement in conventional heat sink designs. Kubo, et al.,[12] explored the correlation between pressure loss and heat transfer coefficients in boiling flows within printed circuit heat exchangers with semicircular and circular mini-channels. Their research established important relationships for design optimization in two-phase flow systems, which offer substantially higher heat transfer coefficients compared to single-phase systems. Said, et al.,[13] conducted a 3D numerical investigation of heat transfer performance in liquid-liquid Taylor flow. Their findings highlighted the enhanced mixing and heat transfer characteristics of segmented flows, providing insights for applications requiring high heat flux dissipation.Cardone&Gargiulo[14]designed and experimentally tested a mini-channel heat exchanger made through additive manufacturing. Their work demonstrated the potential of 3D printing technologies to create complex channel geometries that would be difficult or impossible to manufacture using conventional methods. This approach opens new possibilities for geometric optimization and functional integration. Dixit, et al.,[15] explored the latest advancements in electronic system cooling with a focus on minichannel heat sink solutions. Their work highlighted how modern manufacturing techniques enable more complex and efficient designs, pushing the boundaries of thermal management capabilities. Kim, et al.,[16] presented an innovative machine learning approach for predicting heat transfer characteristics in micro-pin fin heat sinks. By developing predictive models based on experimental and computational data, they demonstrated how artificial intelligence could accelerate design optimization and reduce the need for extensive prototyping. The reviewed literature demonstrates promising pathways toward more efficient and compact thermal management solutions for next-generation electronic systems. The literature reveals the ongoing challenge remains to balance thermal performance with pressure drop, manufacturing complexity, and system integration requirements. However, the reviewed literature demonstrates promising pathways toward more efficient and compact thermal management solutions for next-generation electronic systems.

The current research proposes a machine learning regression based Reynolds number examination for predicting and optimizing heat sink performance in minichannels interrupted.The novelty of the research is that it examines two microchnnelsi. Rectangular and V-type chamber interrupted minichannel heat sink. CFD numerical simulations are carried out on rectangular and V-type chamber interrupted minichannel heat sink by using ANSYS Fluent 21.0.Reynolds number (Re), Nusselt number (Nu),heat transfer coefficient (h) are calculated by CFD numerical simulations. Based on the readings six machine learning regression models namely Linear Regression, Ridge Regression, Lasso Regression, Random Forest, Gradient Boosting, Support Vector Regression (SVR) are developed by using Python. Developed regression models used to predict Nusselt number (Nu) and heat transfer coefficient (h).

2. Methodology and Numerical Simulation

2.1Methodology

The methodology adopted in this research consists of the following steps

1. Description of the interrupted rectangular and V shape minichannel heat sink, boundary conditions, and assumptions.
2. CFD based numerical simulation approach is carried out by using ANSYS Fluent 21.0.
3. Description of the boundary conditions, and assumptions required for CFD analysis.
4. Development of six machine learning models Gradient Boosting, Support Vector Regression (SVR), and Ridge Regression, alongside Random Forest, Linear Regression and Lasso Regression are developed by using Python.
5. A thorough error analysis on Reynolds-Nusselt number correlation to validate the data and assess its reliability is carried out.

2.2 Geometrical Model and Numerical Analysis

2.2.1 Description of Interrupted Mini-Channel Heat Sink

Two aluminium heat sink designs with interrupted mini-channel configurations one with rectangular interruptions and another with V-type interruptions are shown in figure 1(a and b) and figure2 (a and b). Aluminum blocks as a base material is considered for both the geometry. The block dimensions 25.4 mm in length, 25.4 mm in breadth, and 10 mm in height overall. Number of minichannels per geometry are 10. Hydraulic diameter is 934 µm. Channel pitch is 1.47 mm between adjacent mini-channels.Both designs feature interruptions that divide each longitudinal mini-channel into three separate zones Interruption pitch is 6.35 mm between transverse chambers. In this study Three different interruption widths were considered for numerical simulation namely 300µm (corresponding aspect ratio= 5.07), 339µm (corresponding aspect ratio= 5.59), 534µm (corresponding aspect ratio= 5.46). Table 1 depicts the overall dimensions of the simple MCHS and the interrupted Rectangular and V-type

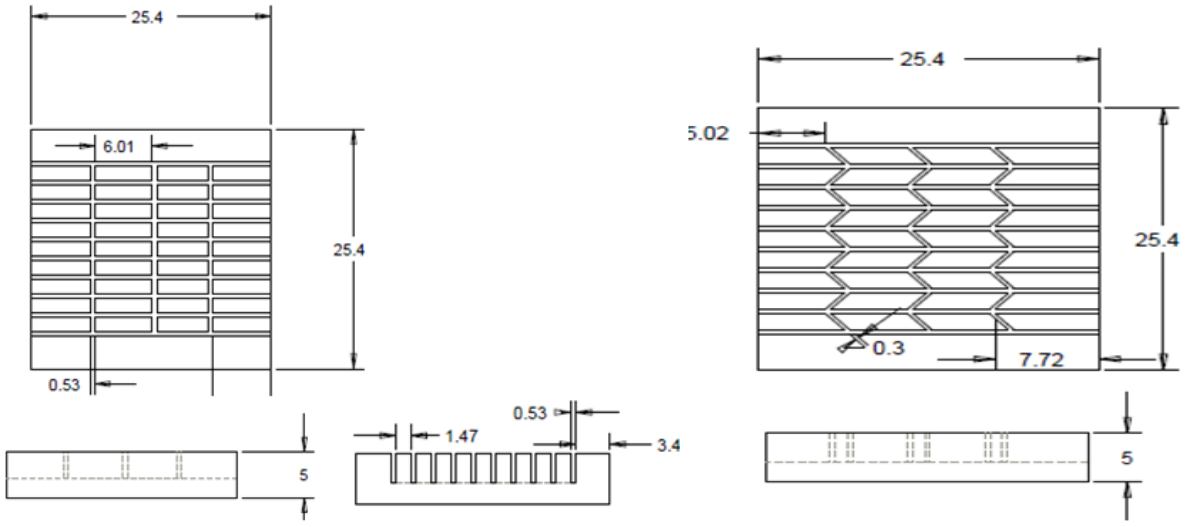

(a) **(b)**

Figure 1. Interrupted Minichannel heat sink (a) Rectangular interrupted geometry (b) V-type interrupted geometry

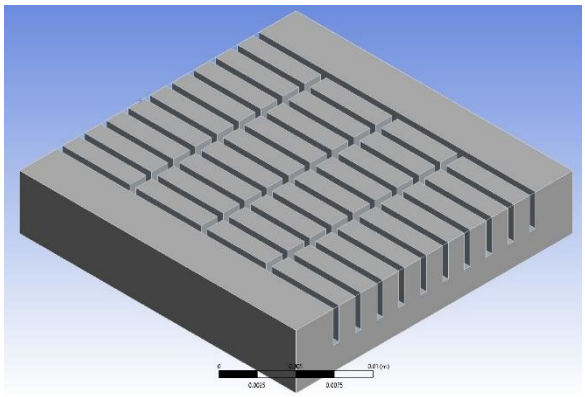

Figure 2 (a) Rectangular interrupted geometry

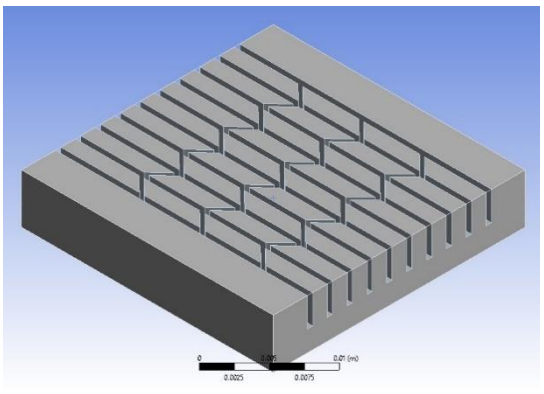

(b) V-type interrupted geometry

Table 1. Geometrical parameters of interrupted Rectangular and V-type minchannels

No. of Channels	Widh (w)μm	Height(b) μm	Width of interrupted Channel(c) μm	Length(L) mm	Hydraulic Diameter (D_h) μm
10	534	2910	300	25.4	903
10	534	2910	339	25.4	903
10	534	2910	534	25.4	903

2.2.2 Governing Equations

The numerical analysis utilized for this study depends on the solution of the mass, momentum, and energy conservation equations in three dimensions. The present work made some assumptions in order to simplify the analysis of heat transfer in microchannel heat sinks (MCHS) are as follows

I. The system operates under steady-state environment
II. The flow is laminar.
III. The fluid is incompressible.
IV. Axial conduction and viscous dissipation are negligible.
V. Fluid properties remain constant, and
VI. Both natural convective and radioactive heat exchange from the mini-channel heat sink are considered negligible. A three-dimensional conjugate heat transfer numerical simulation was carried out to analyze the characteristics of fluid flow and the aluminum channel heat sink.

The governing equations in X, Y, Z direction are expressed as follows[13];

Continuity equation;

$$\frac{\partial V_x}{\partial X} + \frac{\partial V_y}{\partial Y} + \frac{\partial V_Z}{\partial Z} = 0$$

Momentum equation;

$$V_X \frac{\partial V_x}{\partial X} + V_Y \frac{\partial V_x}{\partial Y} + V_Z \frac{\partial V_x}{\partial Z} = -\frac{1}{\rho_{cf}} \frac{\partial P}{\partial X} + \nu_{cf} \nabla^2 V_X$$

$$V_X \frac{\partial V_y}{\partial X} + V_Y \frac{\partial V_y}{\partial Y} + V_Z \frac{\partial V_y}{\partial Z} = -\frac{1}{\rho_{cf}} \frac{\partial P}{\partial Y} + \nu_{cf} \nabla^2 V_Y$$

$$V_X \frac{\partial V_y}{\partial X} + V_Y \frac{\partial V_y}{\partial Y} + V_Z \frac{\partial V_y}{\partial Z} = -\frac{1}{\rho_{cf}} \frac{\partial P}{\partial Z} + \nu_{cf} \nabla^2 V_Z$$

Energy equation;

$$V_X \frac{\partial T}{\partial X} + V_Y \frac{\partial T}{\partial Y} + V_Z \frac{\partial T}{\partial Z} = \frac{\lambda_{cf}}{\rho_{cf} C_{P,cf}} \nabla^2 T$$

2.2.3Boundary Conditions

Water is utilized as the working fluid within the fluid domain to facilitate heat rejection through conventional heat transfer mechanisms. The fluid enters the inlet surfaces with a velocity normal to the inlets, ranging between 0.08547 m/s and 0.42735 m/s, corresponding to mass flow rates varying from 0.0056 kg/s to 0.0278 kg/s. The fluid exits the system at atmospheric pressure (1 atm). To ensure the absence of fluid movement or heat transfer across periodic boundary surfaces, adiabatic boundary conditions are imposed on the fluid domain's top and side surfaces. At the inlet, both temperature and velocity are maintained constant, while atmospheric pressure is specified at the outlet as the boundary condition.

2.2.4 Numerical Scheme and Convergence Criteria

The finite volume approach was used to solve governing equation based on commercial program ANSYS Fluent 21.0. Depending on the hydraulic diameter of the channels, the Reynolds number ranged between 100 and 600. The semi-implicit algorithm known as SIMPLEC (Semi-Implicit Method for Pressure Linked Equations–Consistent) was employed for coupling pressure and velocity fields. For discretizing momentum and energy equations, a second-order upwind scheme was utilized, while the pressure term was also discretized using a second-order approach. The convergence criteria were established by setting residual values at 10^{-6} for continuity and velocities in the x, y, and z directions, and 10^{-7} for energy equations. The control volume was created by dividing the geometry into smaller elements through mesh generation, emphasizing that the accuracy and computational efficiency of numerical simulations are significantly influenced by mesh quality, element shape, and size distribution. Thus, selecting an appropriate meshing strategy effectively reduces computational time for each simulation.

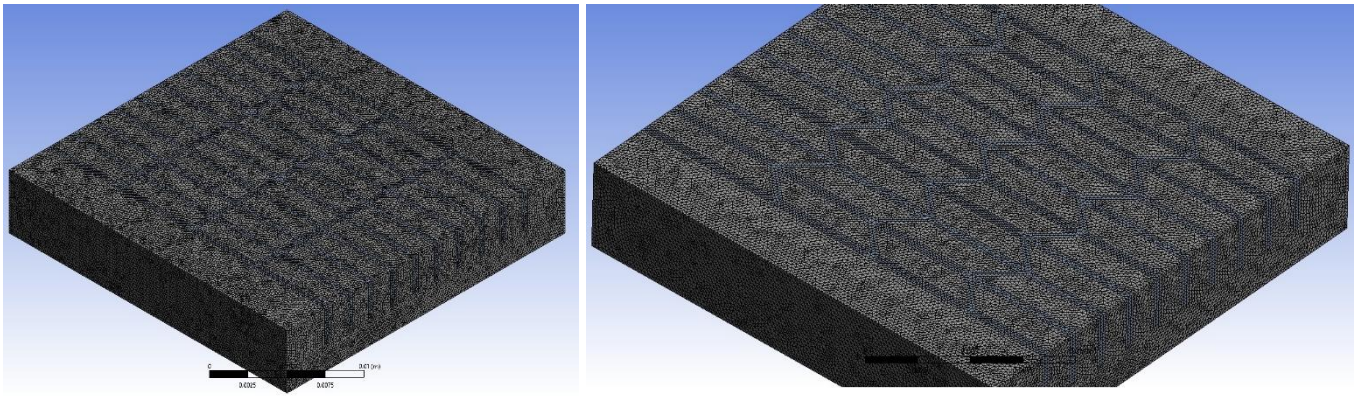

Figure 3. (a) Rectangular shape meshing (b) V Shape meshing

Figure 3(a and b) provides a three-dimensional mesh visualization that distinguishes between the two computational domains clearly (fluid and solid) of the interrupted rectangular structure. Details in the circumstances examined in this study necessitate the employment of a mesh of the tetrahedron type. Compared to quadratic elements, tetrahedrons can produce more cells with the same mesh size. For reasonably complex geometry like corner angles, channels, and grooves, this approach works best. The network was purified for every case based on a deviation measure that produced 0.799 ± 0.001. Table 1 represents Fluent Parameter implemented in this CFD analysis.

Table 1. Fluent Parameter

Parameters	Conditions	Value
Mesh scale	Aspect Ratio	1.05287e+01
Mesh Type	Tetrahedral	
Model	Energy Equation	Viscous Laminar model
Solid material	Aluminium	Density-2719, Cp – 871,K – 202.4

Fluid material	Water	4.187
Boundary conditions Inlet	Velocity inlet	0.0394,Normal to Boundry
Outlet	Pressure	0 Pa , Normal to Boundary
Heaters	Heat flux	32000 W/m^2
Run Calculation	Standard Initialisation	Relative to Cell Zone

2.3 Machine Learning

In contemporary research, as mention Table 1 heat sink performance prediction utilizes eight key input parameters: heat sink geometric configuration (Shape), Reynolds number (Re), input temperature (Ti), output temperature (To), surface temperature (Ts), average temperature between inlet and outlet (Tf), wall temperature differential (ΔTw), and mass flow rate (m). The models target three output variables: Heat transfer (Q), Heat transfer coefficient (h), and Nusselt number (Nu). Implementation was conducted using Python-based machine learning tools with a dataset comprising 430 total inputs. The dataset was partitioned into training (80%) and testing (20%) segments. Comparative analysis of various algorithms—including Gradient Boosting, Support Vector Regression (SVR), and Ridge Regression, alongside Random Forest, Linear Regression and Lasso Regression —revealed that the Gradient Boosting model demonstrated superior performance. Consequently, the Gradient Boosting algorithm was selected for the prediction and optimization of heat sink performance in interrupted minichannels.

Table 2. Machine learning Input and output parameters

Sr. No.	Machine Learning Model	Input Parameters	Out Variables
1	Linear Regression	Shape, Re, Ti, To, Ts, Tf, ΔTw, m	Q, h, Nu
2	Ridge Regression		
3	Lasso Regression		
4	Random Forest		
5	Gradient Boosting		
6	Support Vector Regression		

3. Results and discussion

3.1 Discussion on findings of Numerical Simulation

In this work 42 numerical simulations are carried out on shape, width of interrupted Channel and Reynolds number. Main focus of numerical simulation is to analyses pressure drop, thermal performance and velocity performance for simple and Interrupted Mini-Channel Heat Sink.The subsequent sections will detail the findings obtained from these simulations. After simulation various parameters such as convective heat transfer coefficient (h), Nusselt number (N_u) were calculated by using following formulas [2],

$$h = \frac{Q}{A\Delta T}$$

$$N_u = \frac{h\, D_h}{K_f}$$

K_f = 4.187 for water

3.1.1Pressure Drop Analysis forInterrupted Mini-Channel Heat Sink

The analysis of pressure drop in both conventional and interrupted mini-channel heat sink designs provides critical insights into system performance. Pressure drop represents the reduction in pressure as fluid navigates through or around pin fin arrangements, primarily affected by fin geometry, fluid velocity, and fluid properties. Selected pressure drop contours from 42 simulations are showcased in Figures 3a-b, illustrating how rate flow and fin configuration affect pressure distribution across the heat sink structure. The V534 design exhibits higher entrance pressure, particularly near leading edges, compared to the R534 design. Pressure consistently decreases as flow progresses

downstream, confirming the expected pressure gradient across the domain. Research findings indicate that V-shaped structures generate flow separation and recirculation that rectangular shapes don't, enhancing turbulence and heat transfer efficiency. Near the V-cut edges, localized pressure variations indicate vortex formation, which improves mixing and cooling performance. The evenly distributed pressure contours suggest well-balanced flow patterns beneficial for efficient cooling, though some pressure fluctuations near interruptions indicate localized effects. Overall, the V-shaped modifications create vortices that significantly improve convective heat transfer compared to both conventional straight fins and rectangular geometries, with the V-type interrupted mini-channel configuration demonstrating superior heat transfer characteristics.

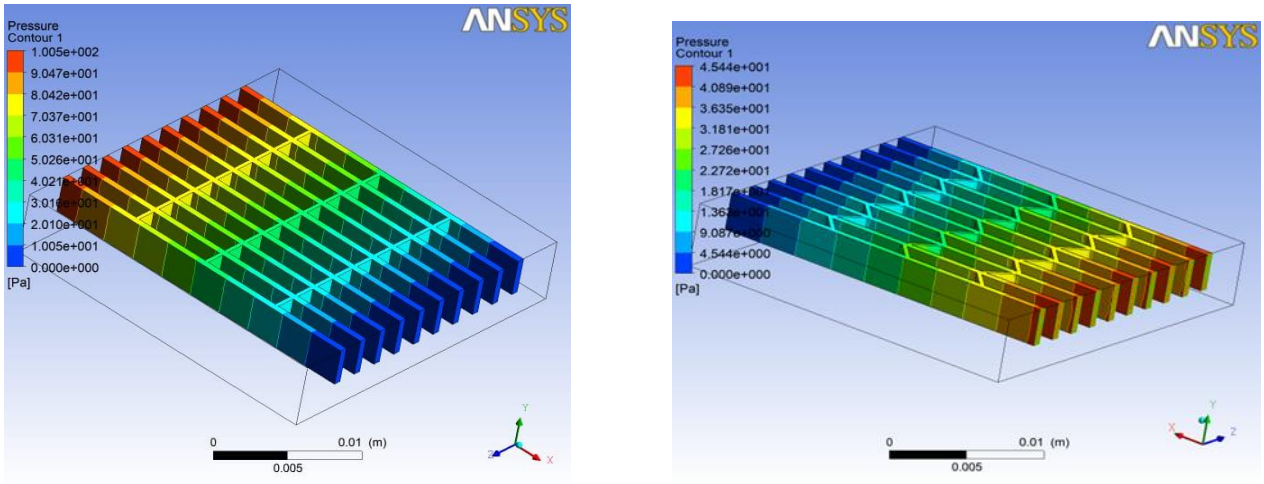

Figure 3. CFD Pressure contour of (a) R 534 shape (b) V_534 shape

3.2.2 Thermal analysis for Interrupted Mini-microchannel Heat Sink

In thermal analysis of mini-microchannel heat sinks, it is essential to investigate how variations in heat source temperature affect the heat exchange characteristics and overall thermal performance of both conventional and interrupted mini-channel heat sink configurations[17]. Figure 4 a-b illustrate the temperature contoursfor R534 shape and V534 shape.

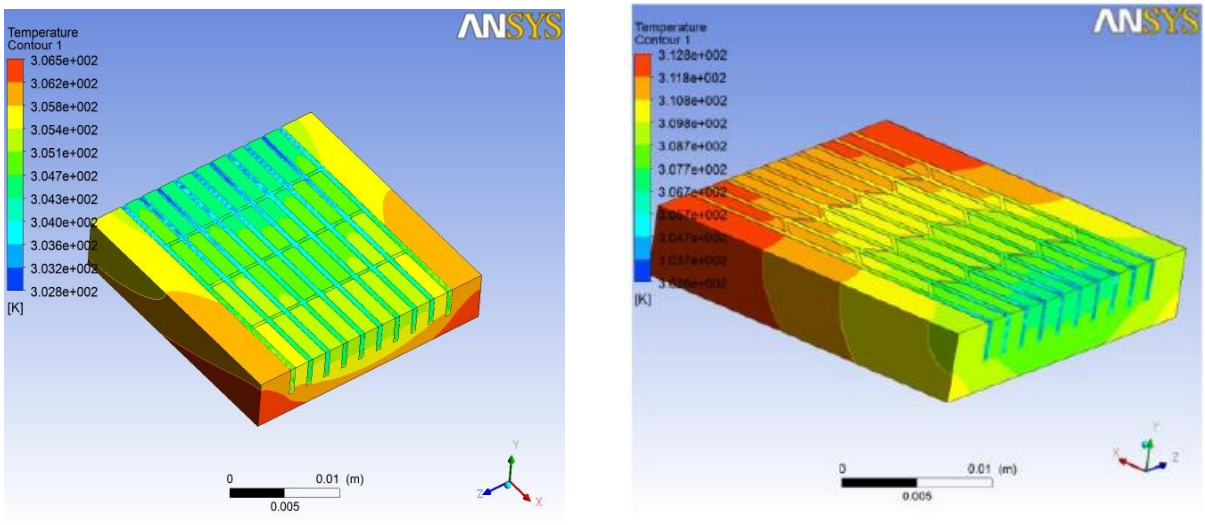

Figure 4.CFD Temperature contour of (a) rectangular 534 shape (b) V_534 shape

In case of V shape, the heat source is at the base, and cooling occurs as the fluid moves through the interrupted channel structure as compared to R shape and conventional shape. The gradual color transition from hot (red/yellow) to cold (green/blue) shows a steady cooling effect. This confirms that heat is effectively conducted through the structure and removed by convection. The V-type interrupted min channels create flow disturbances, improving mixing and heat dissipation. Increased turbulence enhances the Nusselt number, leading to higher convective heat

transfer. The temperature gradient suggests that heat is evenly distributed over the geometry. This is beneficial for thermal management applications like electronics cooling and heat exchangers.

3.2.3Nusselt number (Nu) and Convective heat transfer coefficient (h) variation with Reynolds number (Re) and width

Variation of Nusselt number (Nu) and convective heat transfer coefficient (h) with Reynolds number (Re) and width for conventional and interrupted mini-microchannel heat Sink is Shown in Table 3. Across all heat sink geometries, the Nusselt number (Nu) shows steep increase with increase in Reynolds number (Re), indicating enhanced convective heat transfer at higher flow rates. This trend suggests that increasing the flow velocity improves heat dissipation, as expected from convective heat transfer principles. Also Theheat transfer coefficient (h) shows positive correlation with Reynolds number, similar to Nu. This indicates that as fluid velocity increases, convective heat transfer improves, reducing thermal resistance.

Table 3.Nusselt number (Nu) and Convective heat transfer coefficient (h) variation with Reynolds number (Re) and width

Sr. No	Shape	Re	Ti	To	Ts	ΔTw	Tf	ΔTw	Time	m	Q	h	Nu
1	R300	100	303.0	311.12	313.00	8.12	307.06	5.94	650	0.00061	20.8127	2168.909	6.15
2	R300	200	303.0	307.12	309.97	4.12	305.06	4.91	325	0.00122	21.0152	2542.254	8.81
3	R300	300	303.0	306.00	309.15	3.00	304.50	4.65	228	0.00170	21.3128	2656.853	10.13
4	R300	400	303.0	305.13	308.48	2.13	304.07	4.41	165	0.00244	21.8195	2756.416	11.63
5	R300	500	303.0	304.76	308.18	1.76	303.88	4.30	132.9	0.00305	22.4906	2788.459	12.76
6	R300	600	303.0	304.51	307.97	1.51	303.76	4.21	111	0.00366	23.1793	2814.942	13.79
7	R339	100	303.0	311.28	313.00	8.28	307.14	5.86	650	0.00061	21.2115	2168.909	6.45
8	R339	200	303.0	307.27	309.97	4.27	305.14	4.83	325	0.00122	21.7983	2542.254	9.41
9	R339	300	303.0	306.15	309.15	3.15	304.58	4.57	228	0.00170	22.4006	2656.853	10.97
10	R339	400	303.0	305.29	308.48	2.29	304.14	4.34	165	0.00244	23.3796	2756.416	12.85
11	R339	500	303.0	304.91	308.18	1.91	303.96	4.22	132.9	0.00305	24.4373	2788.459	14.37
12	R339	600	303.0	304.66	307.97	1.66	303.83	4.14	111	0.00366	25.5147	2814.942	15.84
13	R534	100	303.0	311.35	313.00	8.35	307.18	5.82	650	0.00061	21.4106	2314.681	6.40
14	R534	200	303.0	307.35	309.97	4.35	305.18	4.79	325	0.00122	22.1839	2834.345	9.61
15	R534	300	303.0	306.22	309.15	3.22	304.61	4.54	228	0.00170	22.8934	3056.926	11.27
16	R534	400	303.0	305.36	308.48	2.36	304.18	4.30	165	0.00244	24.1323	3325.374	13.44
17	R534	500	303.0	304.98	308.18	1.98	303.99	4.19	132.9	0.00305	25.2953	3493.390	14.97
18	R534	600	303.0	304.73	307.97	1.73	303.87	4.10	111	0.00366	26.5353	3657.797	16.50
19	V300	100	303.0	310.74	313.00	7.74	306.87	6.13	650	0.00061	19.8368	2348.569	5.66

20	V300	200	303.0	306.78	309.97	3.78	304.89	5.08	325	0.00122	19.2638	2870.424	7.71
21	V300	300	303.0	305.68	309.15	2.68	304.34	4.81	228	0.00170	19.0633	3071.395	8.63
22	V300	400	303.0	304.84	308.48	1.84	303.92	4.56	165	0.00244	18.7690	3312.698	9.51
23	V300	500	303.0	304.45	308.18	1.45	303.73	4.45	132.9	0.00305	18.5269	3507.197	9.56
24	V300	600	303.0	304.20	307.97	1.20	303.60	4.37	111	0.00366	18.3553	3687.421	10.27
25	V339	100	303.0	310.74	313.00	7.74	306.87	6.13	650	0.00061	19.8368	2425.333	5.81
26	V339	200	303.0	306.78	309.97	3.78	304.89	5.08	325	0.00122	19.2638	3024.717	8.03
27	V339	300	303.0	305.68	309.15	2.68	304.34	4.81	228	0.00170	19.0633	3282.141	9.10
28	V339	400	303.0	304.84	308.48	1.84	303.92	4.56	165	0.00244	18.7690	3611.966	10.27
29	V339	500	303.0	304.45	308.18	1.45	303.73	4.45	132.9	0.00305	18.5269	3879.541	11.01
30	V339	600	303.0	304.20	307.97	1.20	303.60	4.37	111	0.00366	18.3553	4133.622	11.56
31	V534	100	303.0	311.05	313.00	8.05	307.03	5.97	650	0.00061	20.6333	2464.436	6.05
32	V534	200	303.0	307.08	309.97	4.08	305.04	4.93	325	0.00122	20.8284	3102.520	8.59
33	V534	300	303.0	305.99	309.15	2.99	304.49	4.66	228	0.00170	21.2368	3379.947	9.93
34	V534	400	303.0	305.14	308.48	2.14	304.07	4.41	165	0.00244	21.8867	3760.140	11.46
35	V534	500	303.0	304.75	308.18	1.75	303.88	4.30	132.9	0.00305	22.4170	4047.959	12.44
36	V534	600	303.0	304.50	307.97	1.50	303.75	4.22	111	0.00366	23.0213	4333.816	13.44
37	Basic	100	303.0	310.81	310.55	7.81	306.91	3.65	650	0.00061	20.0162	2147.220	5.54
38	Basic	200	303.0	306.81	307.50	3.81	304.91	2.60	325	0.00122	19.4505	2516.832	7.56
39	Basic	300	303.0	305.69	306.66	2.69	304.35	2.31	228	0.00170	19.1394	2630.285	8.35
40	Basic	400	303.0	304.83	305.99	1.83	303.91	2.08	165	0.00244	18.7025	2728.852	9.08
41	Basic	500	303.0	304.46	305.69	1.46	303.73	1.97	132.9	0.00305	18.6010	2760.574	9.54
42	basic	600	303.0	304.21	305.49	1.21	303.60	1.88	111	0.00366	18.5133	2786.793	9.91

Figure 5 shows Effect of Reynolds Number and width of conventional and interrupted (Rectangular and V- type) mini-channels on Nusselt number (Nu).Compare to conventionaland R shape V Shape interrupted MCHS Show a gradual increase in Nu with Re. The variation among different shapes implies that geometry significantly affects heat transfer efficiency. V-type shapes provide higher Nusselt numbers for the same Reynolds number, meaning they enhance convective heat transfer more effectively. At low Reynolds numbers (Re < 500), differences between shapes are less pronounced, as laminar flow dominates. At higher Reynolds numbers (Re > 500), Nu differences become significant with V-type interrupted MCHS showing the best performance and rectangular fins showing the least enhancement.V_534 show a steeper rise in Nu, indicating better heat transfer efficiency.Other shapes display a gradual increase, meaning they rely more on conduction rather than convective effects.

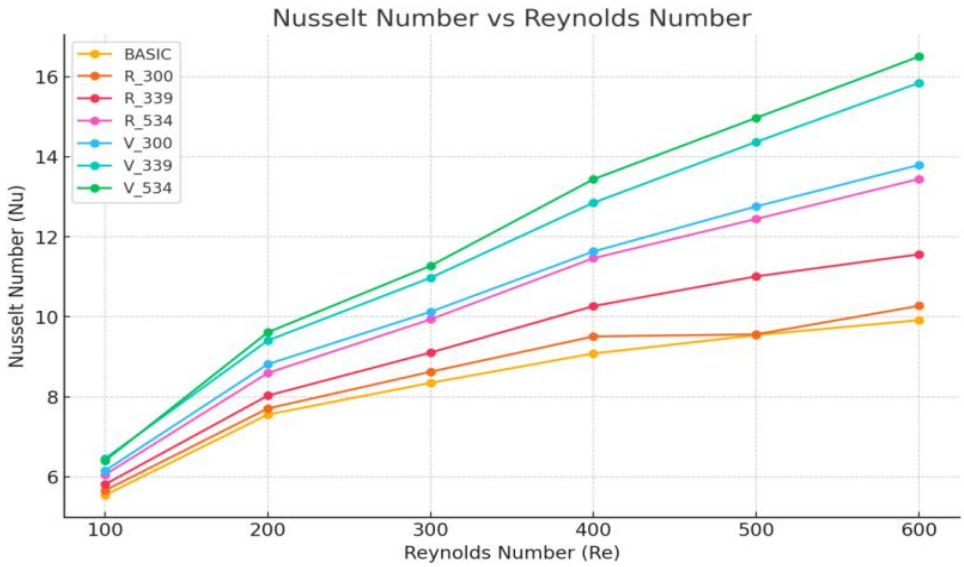

Figure 5. Effect of Reynolds Number and width of interrupted (Rectangular and V- type) mini-channels on Nusselt number (Nu)

Figure 6 shows Effect of Reynolds Number and width of conventional and interrupted (Rectangular and V- type) mini-channels on Heat transfer coefficient.Compare to conventional and R shape V Shape interrupted MCHS Showheat transfer coefficient (h) increases with Re, confirming improved heat transfer performance at higher velocities. The v534 shape has the highest h values, making it the best design for maximizing overall heat dissipation. The v339 shape balances both Nu and h, making it the most versatile option.

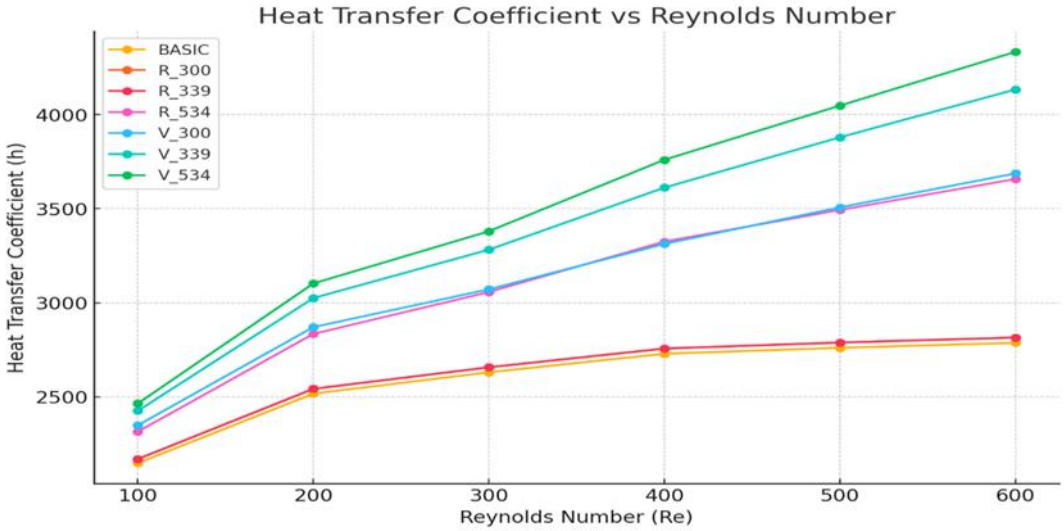

Figure 6. Effect of Reynolds Number and width of interrupted (Rectangular and V- type) mini-channels on Heat transfer coefficient

3.3 Discussion on findings of Machine Learning Models

In the current research, the train machine learning models namely Gradient Boosting, Support Vector Regression (SVR), and Ridge Regression, alongside Random Forest, Linear Regression and Lasso Regression are employed for predicting and optimizing heat sink performance in Interrupted minichannels along with determination of machine learning models predicting and optimizing accuracy.After training and testing of the machine learning models as mentioned in Table 4 and shown figure 7, it is found that Gradient Boosting model demonstrated superior performance than other models [17, 18].

Table. 4 Performance of train machine learning models

Model	MAE (Nu)	MSE (Nu)	R^2 Score (Nu)	MAE (h)	MSE (h)	R^2 Score (h)
Linear Regression	0.453	0.289	0.82	254.67	50236.22	0.76
Ridge Regression	0.431	0.275	0.85	238.34	48321.18	0.79
Lasso Regression	0.472	0.312	0.80	267.89	51564.09	0.74
Random Forest	0.223	0.091	0.94	124.55	22589.36	0.92
Gradient Boosting	0.198	0.075	0.97	98.77	18456.45	0.95
Support Vector Regression (SVR)	0.412	0.268	0.83	232.19	47612.34	0.78

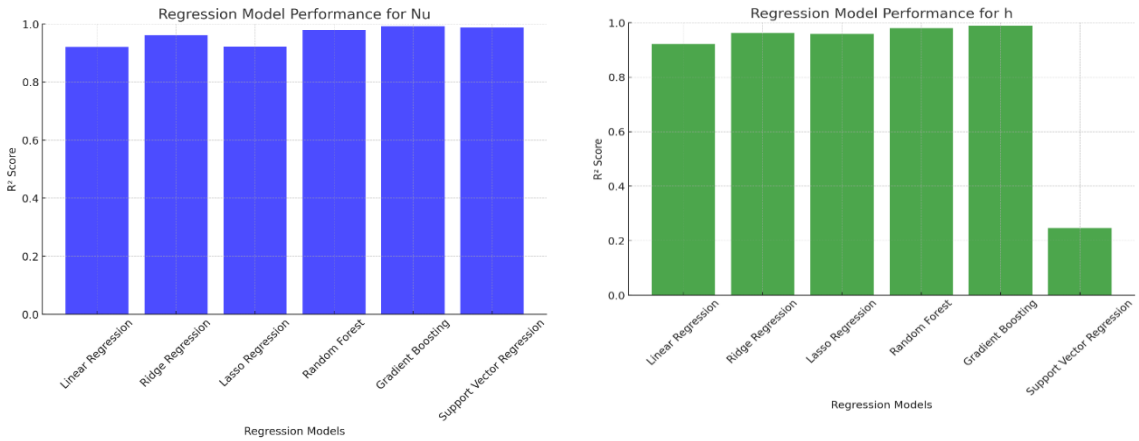

(a) (b)

Figure 7.Regression Analysis (a) Nusselt number (Nu) (b) Heat Transfer Coefficient (h)

4. Conclusion

In the current research paper, CFD numerical simulation was performed on the conventional and interrupted (Rectangular and V- type) mini-channels. Further, six machine learning models namely Gradient Boosting, Support Vector Regression (SVR), and Ridge Regression, alongside Random Forest, Linear Regression and Lasso Regression are developed for predicting and optimizing heat sink performance in Interrupted minichannels along with determination of machine learning models predicting and optimizing accuracy. Based on numerical simulation and the machine learning model, subsequent conclusions have been drawn;

I. The computational fluid dynamics (CFD) investigation revealed significant performance differences among conventional, rectangular, and V-type interrupted mini-channel heat sinks (MCHS). The V534 configuration demonstrated superior thermal performance, exhibiting a more pronounced increase in Nusselt number (Nu) compared to other geometries, indicating enhanced convective heat transfer rather than conduction-dominated processes.

II. For the V534 design specifically, the convective heat transfer coefficient (h) showed strong positive correlation with Reynolds number (Re), confirming enhanced thermal performance at higher flow velocities relative to conventional and rectangular configurations. The V534 design consistently achieved the highest h values, establishing it as the optimal configuration for maximizing heat dissipation efficiency.

III. Analysis across all tested geometries confirmed that both Nu and h increase with Re, validating that elevated flow rates enhance convective heat transfer mechanics. The varying responses of different geometries across Re ranges underscore the critical role of channel configuration in thermal performance optimization.

IV. Machine learning model evaluation, including Linear Regression, Ridge Regression, Lasso Regression, Random Forest, Gradient Boosting, and Support Vector Regression (SVR), identified the Gradient Boosting algorithm as the most accurate predictive model for both Nu and h parameters, demonstrated by its superior R^2 scores and minimal error metrics.

V. The comprehensive research findings indicate that heat sink geometry selection substantially influences thermal performance characteristics, Reynolds number demonstrates direct proportionality with both Nu and h, and the V534 configuration provides the optimal balance between thermal efficiency and heat dissipation capability for practical applications.

References

[1] Dixit T, Ghosh I. Review of micro- and mini-channel heat sinks and heat exchangers for single phase fluids. Renew. Sustain. Energy Rev. 2015, p. 1298–1311. doi: 10.1016/j.rser.2014.09.024

[2] Datta A, Sanyal D, Agrawal A. Das AK. A review of liquid flow and heat transfer in microchannels with emphasis to electronic cooling. Sadhana. 2019, p. 1-32. https://doi.org/10.1007/s12046-019-1201-2

[3] Yu H, Li T, Zeng X, He T, Mao N. A Critical Review on Geometric Improvements for HeatTransfer Augmentation of Microchannels. Energies. 2022, p. 1-45. https://doi.org/10.3390/en15249474

[4] Zheng S, Feng Z, Lin Q, Hu Z, Lan Y, Guo F, Huang K, Yu F.Numerical investigation on thermal–hydraulic characteristics in a mini-channel with trapezoidal cross-section longitudinal vortex generators. Appl. Therm. Eng. 2022, p. 1-12.doi: 10.1016/j.applthermaleng.2021.118004

[5] Upadhyay MK, Singh AK, Mishra P. Numerical Investigation On The Heat Transfer In Micro-Channels With Trapezoidal Ribs- A Review. International Journal of Creative Research Thoughts. 2023; p. 1-5.

[6] Xu S, Yang L, Li Y, Wu Y, Hu X. Experimental and numerical investigation of heat transfer for two-layered microchannel heat sink with non-uniform heat flux conditions. Heat Mass Transf. 2016, p. 1755–1763. doi: 10.1007/s00231-015-1691-3

[7] Naqiuddin NH, Saw LH, Yew MC, Yew MK, Yusof F. Numerical study of the geometrically graded micro-channel heat sink for high heat flux application. Energy Procedia. 2017, p. 4016–4021. doi: 10.1016/j.egypro.2017.12.319

[8] Naqiuddin NH, Saw LH, Yew CM, Yusof F, Poon HM, Cai Z, Thiam HS. Numerical investigation for optimizing segmented micro-channel heat sink by Taguchi-Grey method. Appl. Energy. 2018, p. 437–450. doi: 10.1016/j.apenergy.2018.03.186

[9] Liu X, Yu J. Numerical study on performances of mini-channel heat sinks with non-uniform inlets. Appl. Therm. En*g*. 2016, p. 856–864. doi: 10.1016/j.applthermaleng.2015.09.032

[10] Lori MS, Vafai K. Heat transfer and fluid flow analysis of microchannel heat sinks with periodic vertical porous ribs. Appl. Therm. Eng. 2022, p. 1-12. doi: 10.1016/j.applthermaleng.2022.118059.

[11] Sushma S, Chandrashekar TK, Banapurmath NR, Nagesh SB, Venkatesh R. Enhancement of Heat Transfer Characteristics of Plain Fin Coated With Graphene Nanoparticle. Journal of Mines, Metals and Fuels. 2023; p. 1-9. DOI: 10.18311/jmmf/2022/31313

[12] Kubo Y, Yamada S, Murakawa H, Asano H. Correlation between pressure loss and heat transfer coefficient in boiling flows in printed circuit heat exchangers with semicircular and circular mini-channels. Appl. Therm. Eng. 2022, p. 1-14 doi: 10.1016/j.applthermaleng.2021.117963.

[13] Said M, Bouda NN, Harmand S. 3D Numerical Investigation of Heat Transfer Performance in Liquid-liquid Taylor Flow. Journal of Applied and Computational Mechanics. 2024; 1-22. DOI: 10.22055/jacm.2023.44421.4211

[14] Cardone M, Gargiulo B. Design and experimental testing of a Mini Channel Heat Exchanger made in Additive Manufacturing. Energy Procedia. 2018, p. 932–939. doi: 10.1016/j.egypro.2018.08.092

[15] P. Allirani, R. Jain, S. Shankar Prasd, K. H. Wanjale, A. Amudha and A. Faiz, "Real-Time Depth Map Upsampling for High-Quality Stereoscopic Video Display," 2024 15th International Conference on Computing Communication and Networking Technologies, Kamand, India, 2024, pp. 1-5, doi: 10.1109/ICCCNT61001.2024.10725345.

[16] Kim K, Lee H, Kang M, Lee G, Jung K, Kharangate CR, Asheghi M, Goodson KE, Lee H. A machine learning approach for predictingheat transfer characteristics in micro-pin finheat sinks. International Journal of Heat and Mass Transfer. 2022, p. 1-10. https://doi.org/10.1016/j.ijheatmasstransfer.2022.123087

[17] Narwade, Prashant, Ravindra Deshmukh, Mahesh Nagarkar, and Vijaykumar Sukhwani. Improvement of ride comfort in a passenger car using magneto rheological (MR) damper. Journal of Vibration Engineering & Technologies 10, no. 7, 2022, p. 2669-2676.

[18] Narwade, Prashant, Ravindra Deshmukh, Mahesh Nagarkar, and Milind Bankar. "Modeling and Simulation of a Semi-active Vehicle Suspension system using PID Controller." In IOP Conference Series: Materials Science and Engineering, vol. 1004, no. 1, p. 012003. IOP Publishing, 2020.